BIOCHEMICAL AND BIOPHYSICAL RESEARCH COMMUNICATIONS **239,** 191–196 (1997)
ARTICLE NO. RC977451

Solution Structure by Site Directed Tryptophan Fluorescence in Tear Lipocalin

Oktay K. Gasymov, Adil R. Abduragimov, Taleh N. Yusifov, and Ben J. Glasgow[1]
Department of Pathology and Department of Ophthalmology, UCLA School of Medicine, Los Angeles, California 90095

Received August 21, 1997

The solution structure of the G strand of human tear lipocalin was deduced by site directed tryptophan fluorescence (SDTF). The fluorescent amino acid, tryptophan, was sequentially substituted for each native amino acid in the sequence of the G strand. The fluorescent properties resolved alternating periodicity as predicted for β sheet structure, twists in the β sheet, strand orientation in the lipocalin cavity, and the relative depth of residues in the cavity. A distribution of microstates with various orientations of dipoles in the side chain environments of the G strand revealed mobility on the nanosecond time scale. SDTF is broadly applicable to most proteins and will complement x-ray crystallography, site directed spin labeling by electron paramagnetic resonance (EPR), and nuclear magnetic resonance (NMR) in the determination of solution structure.

Tear lipocalin is the principal lipid binding protein in tears and is bound to fatty acids, glycolipids, phospholipids and cholesterol in tears (1). Its broad ligand specificity makes tear lipocalin an unusual member of the expanding lipocalin family, proteins characterized by the ability to bind small hydrophobic molecules. X-ray crystallography and computer generated models of several lipocalins have revealed structural features in common (2-6). Eight strands are arranged in a β-barrel and are joined by loops between the β strands (2). However, the solution structure of lipocalins has been problematic. β-lactoglobulin is found as a dimer in the native state. But the solution structure of β-lactoglobulin could be obtained by nuclear magnetic resonance (NMR) only in the monomeric form at acidic pH, (4). Three structurally conserved regions have been identified for the lipocalins (2). One of these regions, the G beta strand, consistently contains tyrosine, isoleucine and phenylalanine residues. Crystallographic structure analysis of similar lipocalins, indicates that these residues are in close proximity to ligands (3,7,8). These features suggested to us that this region may be important for ligand binding. We sought to investigate the solution structure of this region.

There are a number of excellent methods for defining structures of proteins. Crystallographic methods provide information about the static structure of proteins. However, no general approach is available for crystallization of membrane proteins. NMR provides solution structure of proteins less than 20 kD but is unfeasible if the protein forms aggregation complexes in solution (4,9). EPR is an exciting technique for revealing solution structure and monitoring structural changes on the millisecond time scale but requires cysteine substitution followed by a spin labeling reaction (10-12). Proteins with multiple cysteines and disulfide bonds or with a deeply buried site in a hydrophobic cavity may require disulfide reduction of the protein before labeling and refolding after labeling. The method that we adopted, SDTF, provides solution structure on the nanosecond time scale but does not require a complex labeling reaction.

In recent years many advances have been made in fluorospectroscopic analysis with tryptophan scanning. Previous work in synthetic peptides has demonstrated resolution of α-helical properties with little pertubational effect by replacement of amino acids with tryptophan (13). A great deal of information about protein structure has been revealed in special cases of proteins bearing one tryptophan but the analysis is made complicated with multiple tryptophan residues (14-18). This led to the hypothesis that sequential substitution of native amino acids by tryptophan followed by tryptophan scanning (SDTF) would reveal information about secondary structure, exposure of individual amino acid residues as well as motion of amino acid residues and neighboring groups.

The rationale for using SDTF to study tear lipocalin structure is multifold. Tryptophan fluorescence is exquisitely sensitive to motion, environment and position

[1] Corresponding author: 100 Stein Plaza, Rm. B-279, Los Angeles, CA 90095. Fax: (310) 794-2144, (310) 825-6998. E-mail: bglasgow@pathology.med.ucla.edu.

0006-291X/97 $25.00

(protein surface or interior) (13,19-21). Therefore, sequential substitution of individual amino acids with tryptophan would yield abundant structural information about each residue in a protein. This approach was well suited for tear lipocalin because it contains a single tryptophan residue in the native structure (6).

MATERIALS AND METHODS

Site-directed mutagenesis and plasmid construction. The tear lipocalin cDNA in PCR II (In Vitrogen, San Diego, CA), previously synthesized (22), was used as a template to clone the TL gene spanning bases 115-592 of the previously published sequence (6) into pET 20 b (Novagene). Flanking restriction sites for NdeI and BamHI were added to produce the native protein sequence as found in tears (23). To avoid the use of subtraction spectra in analysis and to simplify the interpretation of quenching experiments in molecules with substituted tryptophans, it was first necessary to substitute the native tryptophan with an amino acid that did not induce significant structural perturbations. We prepared a tear lipocalin mutant, W17Y with oligonucleotides (Universal DNA Inc.) using the previously published method of introduction of a point mutation by sequential PCR steps (24). Twelve additional mutant cDNAs were constructed in which the corresponding amino acids 94-105, on the G strand of tear lipocalin were converted sequentially to trytophan. (Amino acid 94 corresponds to Lys, bases 394-396 of Redl (6).

Expression and purification of mutant proteins. The mutant plasmids were transformed in E. Coli, BL 21 (DE3) and cells were cultured and protein was expressed according to the manufacturer's protocol (Novagene). Following cell lysis as previous described (25), the supernatant was treated with methanol (40% final concentration) at 4°C for 2 1/2 hours. The suspension was centrifuged at 3000g for 30 minutes. The supernatant was dialysed against 50 mM Tris HCl pH 8.4. The dialysate was treated with ammonium sulfate 45-75% saturation. The resulting precipitate was dissolved in 50 mM Tris HCL pH 8.4 and applied to a Sephadex G-100 column (2.5 × 100 cm) equilibrated with 50 mM Tris HCL, 100 mM NaCl, pH 8.4. The fraction containing the mutant protein was dialysed against 50 mM Tris HCL, pH 8.4 and applied to a DEAE Sephadex A-25 column. Bound protein was eluted with a 0-.8M NaCl gradient. Eluted fractions containing mutant proteins were centrifugally concentrated (Amicon, Centricon-10). Purity of mutant proteins was verified by SDS tricine gel electrophoresis (1). The protein concentration was determined by the biuret method (26).

Circular dichroism measurements. Spectra were recorded (Jasco 600 spectropolarimeter, .2 mm path length for far-UV spectra) using protein concentrations of 1.2 mg/ml. Eight scans from were performed from 190-260 nm. Results were recorded in mdegrees.

Fluorescence spectroscopy. Fluorescence measurements were made on Perkin-Elmer LS-5 specrofluorometer using 3-nm bandwidths except for quenching experiments (5-nm bandwidths). The excitation λ of 295 nm was used to ensure that light was absorbed almost entirely by tryptophanyl groups. Protein solutions with less than .1 OD at 295 nm were analysed. All spectra were obtained from samples in 10mM sodium phosphate, pH 7.3, at room temperature. The fluorescence spectra were corrected for light scattering from buffer. The fluorescence of a protein, monitored at its emissions λ_{max}, was quenched by the progressive addition of small aliquots of an 8M acrylamide solution as previous described (20). Correction for dilution of the sample and for inner filter effects caused by acrylamide absorption was performed as previously described (20). The quenching data were fit to the modified form of the Stern-Volmer relationship (20): $F_o/F=(1+Ksv[Q])e^{V[Q]}$ where F_o and F are the fluorescence intensities in the absence and presence of the quencher, respectively, [Q] is the concentration of quencher, K_{sv} is the dynamic quenching constant and V is the static quenching constant. $K_{sv}=K_q\tau_o$ Estimation of collisional rate constant, K_q, was performed using L-tryptophan as a fluorescence standard. The quantum yield and fluorescence lifetime, τ_o, were assumed to be .13 and 2.8 ns, respectively (27,28). The red excitation experiment was performed according to Demchenko (29) under the conditions above. The parameter I_{320}/I_{360} is a linear function of fluorescence maxima positions. For blue shift effects the parameter I_{320}/I_{360} calculated at acrylamide concentrations of 0 and .7M.

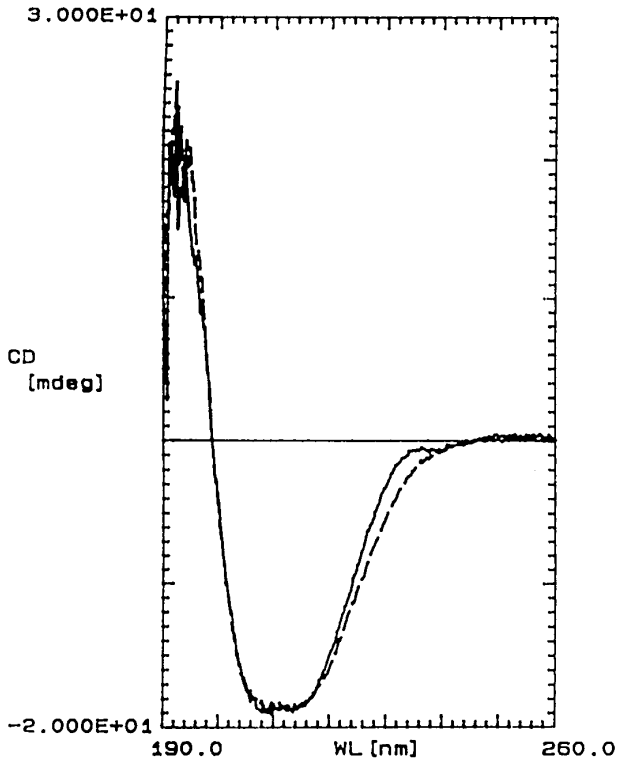

FIG. 1. Far UV CD spectra of expressed proteins. (—) wild type of tear lipocalin; (---) mutant W17Y. Spectra were obtained from protein samples 1.0 mg/ml in 10mM sodium phosphate buffer, pH 7.3.

RESULTS AND DISCUSSION

Circular Dichroism

We compared circular dichroic spectra of expressed W17Y mutant tear lipocalin with that of the wild type. The superimposed far UV CD spectra were extremely similar and showed nearly identical content of β sheet and alpha helical structure confirming the lack of significant secondary structural alterations with this substitution (Fig. 1). The spectra of both samples, indicating β structure, overlap except in the range 218-238 nm where the loss of the positive aromatic side chain contribution of the mutant is evident as greater optical activity. Expressed W17Y mutant tear lipocalins that included sequentially substituted tryptophans for amino acids K94-L105 showed no significant differ-

ences in the far UV CD spectra from the W17Y mutant (data not shown).

Fluorescence

We reasoned that fluorescence spectra of sequentially substituted tryptophans of a β sheet should reflect the periodic physico-chemical environment of amino acids along the peptide chain. Since the lipocalins are composed of β sheets we proposed to study the G strand region of tear lipocalin, K94-L105, that by our calculation and others should contain a β sheet structure (6). Tryptophanyl residues that are exposed to a more polar enviroment (exposed to solvent) and have high mobility reveal maximum emission peaks that are red shifted and those in apolar environment (buried in the protein) would reveal blue shifted emission (19-21).

Analysis of the emission peaks of the fluorescent spectra indicated alternating periodicity of residues F99-L105 in their exposure to solvent as predicted for a β sheet (Figs. 2 and 3). Hence Y100, E102, E104 are oriented exposed to solvent while F99 C101, G103 and L105 are oriented in the interior of the protein.

Furthermore, from the relative emission peaks of the internally situated molecules we hypothesized that the F99 was likely to be deeply buried in the lipocalin cavity while L105 was in a more shallow position. However, positions of the emission peaks are complex and related not only to the exposure of tryptophan in a protein but also to the polarity of its microenvironment as well as to specific interactions with polar groups of the protein, the presence of water molecules in the protein's interior, and mobility (20). In order to obtain a quantitative measure of kinetic exposure of the tryptophans used in substitution we performed acrylamide quenching experiments. The quenching reaction involves physical contact between acrylamide and an excited indole ring and can be kinetically described in terms of a collisional and a static component that are calculated from the modified Stern-Volmer plot (Fig. 4). In the calculations of the dynamic and static components of the quenching reactions there is evidence for β sheet structure. Inspection of Fig. 5 shows alternating periodicity from F99-L105 for both collisional rate constants and static quenching constants. A further examination of the plots shows a progressive increase in collisional rate constants for buried residues from F99 to L105. Since in a perfect β sheet, all buried residues share a similar orientation with respect to the solvent, influences of depth in the cavity and configuration of the β sheet must affect the collisional rate constants. An analogous situation exists for exposed residues. F99 has the lowest collisional rate constant and therefore lies deep in the cavity. L105 is more exposed although still oriented away from solvent and therefore is more shallow position in the cavity. Furthermore, the progressive increase in the collisional rate constants for the even numbered residues exposed to solvent, Y100-E104, indicates that the β sheet is twisted. Unlike the case for buried residues, the collisional rate constant of exposed residues is not limited by diffusion of acrylamide to a position in the cavity but rather by the relative orientation of the residues with respect to solvent molecules. Y100 is turned slightly toward the interior of the cavity and has relatively less exposure than E104 which is turned exteriorly. Both the position of emission peaks and collisional rate constants provide further evidence for twisting of the G strand. Alternate periodicity is predicted by the Chou-Fasman analysis in the region of residues I98 and F99 (6). If the G strand

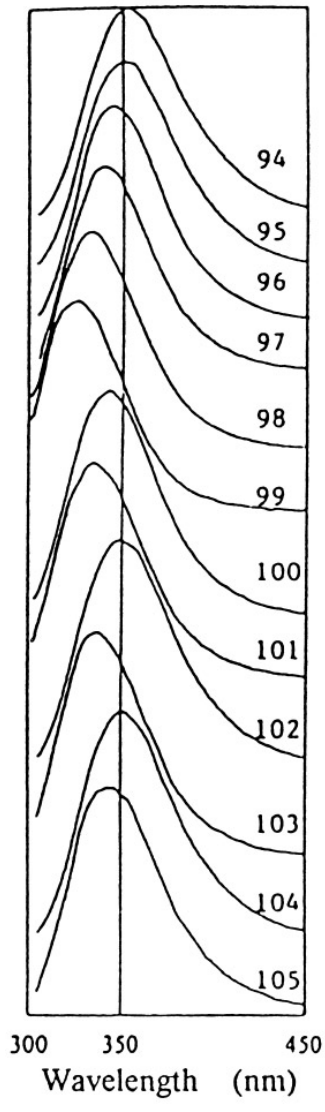

FIG. 2. Fluorescence spectra of expressed mutant tear lipocalin proteins. Spectra were obtained from samples in 10mM sodium phosphate, pH 7.3, at room temperature. The fluorescence intensities of the mutants were adjusted to the same gain.

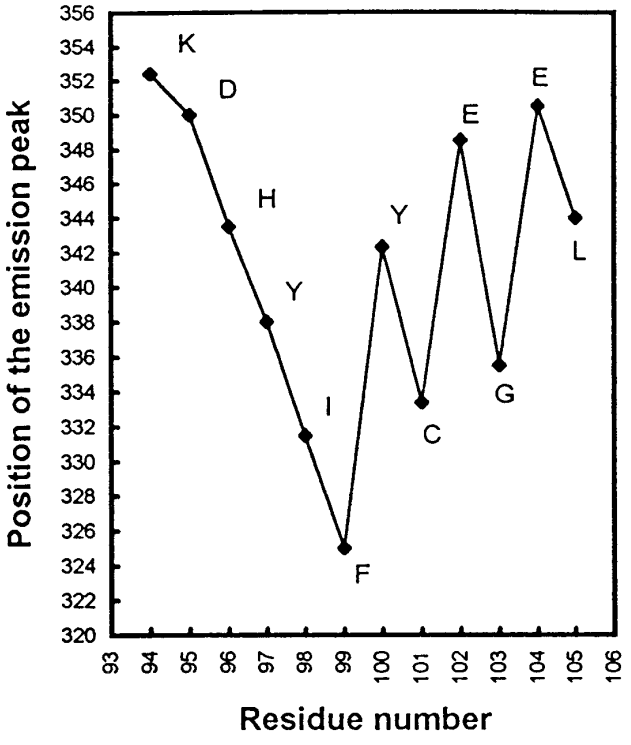

FIG. 3. The position of the emission peak (from above) versus position of the tryptophan substitution in the tear lipocalin sequence.

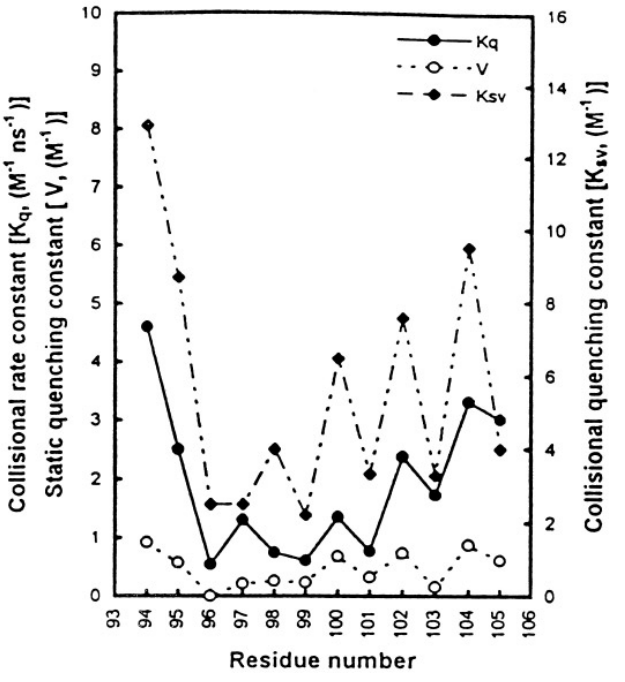

FIG. 5. Fluorescence quenching constants versus position of the tryptophan substitution in the tear lipocalin sequence.

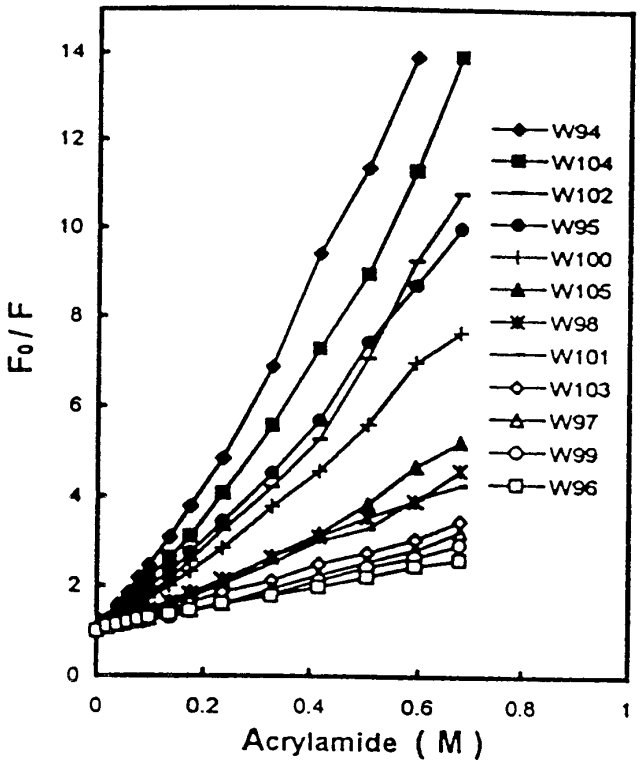

FIG. 4. Stern-Volmer plots of Trp fluorescence quenching by acrylamide at pH 7.3 of tear lipocalin mutants.

were an ideal β structure, I98 would be oriented exposed to solvent. But the collisional rate constant are similar to F99; I98 is not exposed.

The findings by SDTF are comparable to crystallographic findings of the homologous G strand of β lactoglobulin. Residues Y102, L103, and L104 of β lactoglobulin are homologous to Y97, I98, and F99; all lie deep in their respective cavities. In both lipocalins, the G strand is twisted.

Comparison of the collisional rate constant with the position of the emission peak for H96 brings to light the influence of polar side chain interactions. The collisional rate constant is low indicating that the residue is not exposed to solvent but the emission peak is red shifted indicating that H96 encounters a polar environment presumably from protein groups.

One of the advantages of fluorescence spectroscopy is the detection of dynamic structure on the nanosecond time scale (29,30). By exploiting fluorescence spectral shift caused by red edge excitation, information can be acquired about the rigidity of surrounding dipoles for each amino acid residue substituted by tryptophan. The basis of the red edge excitation effect is that inhomogenous chromophore microstates results in broadening of the electronic spectra. When the relaxation time following excitation is longer than the fluorescence lifetime ($\tau_r > \tau_f$), it is possible to detect the altered distribution as a manifestation of motion. The fluorescence spectra for varying excitation wavelengths were measured for all mutants representing sequentially substi-

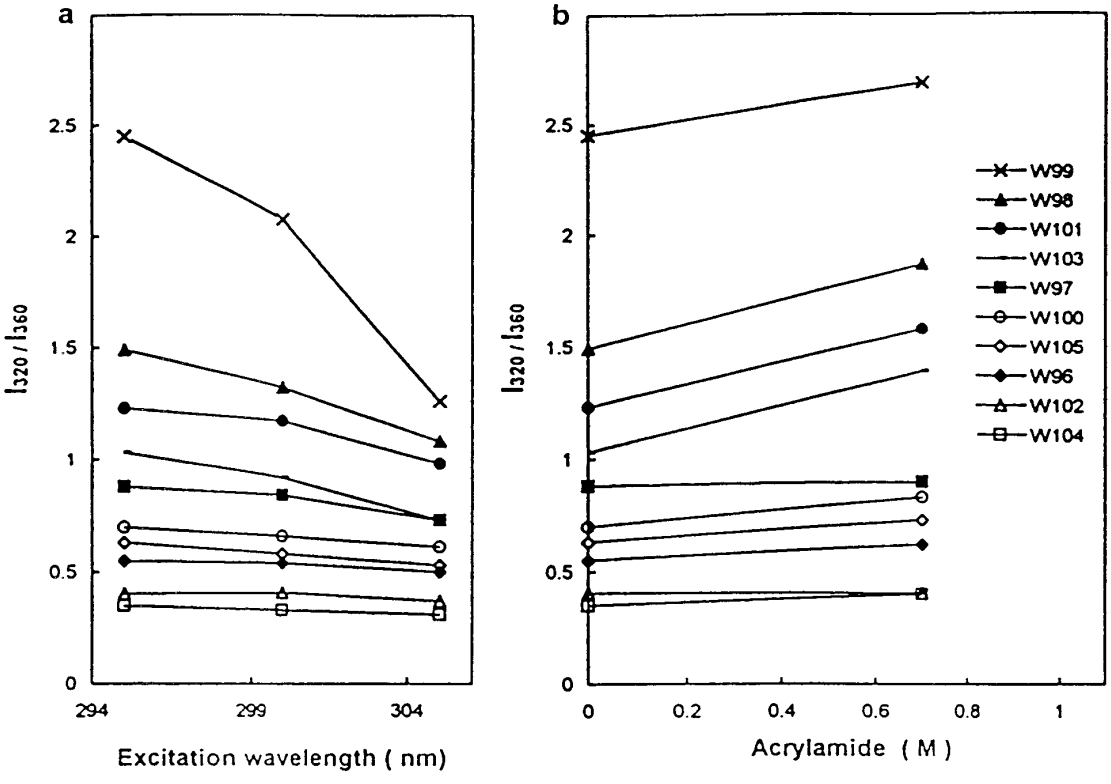

FIG. 6. The red edge excitation and blue shifts for tryptophan substituted mutants. **(A)** I_{320}/I_{360} versus excitation wavelength for tryptophan substituted mutants. **(B)** I_{320}/I_{360} at acrylamide concentrations of 0 and 0.7M.

tuted amino acids with tryptophan (Fig. 6) and the red edge excitation effect for different locations is compared (Fig. 7A). Four mutants, W98, W99, W101, and W103, that are internally located in the cavity showed a prominent red edge excitation effect indicative of a more rigid environmental state. W99, located deep in the cavity, is in the most rigid state. However, W105 is also internally located in the cavity but shows little red excitation effect and therefore must be surrounded by mobile dipoles composed of protein groups. W100, W102, and W104, located external to the cavity, show a minimal red excitation effect, indicative of reorientation of surrounding solvent dipoles on a subnanosecond time scale (29).

Information regarding the relative exposure of the subset of tryptophanyl residues in a rigid state is provided by an analysis of acrylamide induced blue shift (Figs. 6B and 7B). Residues exhibiting the red excitation effect are in a rigid microenvironmental state. The subpopulation of residues that are more exposed and fluoresce at longer wavelengths are preferably quenched leading to a blue shift in the composite spectra. For most of the substituted residues we found that there is a blue shift. However, at the positions W97 and W99 there are blue shifts that are markedly less than the corresponding marked red excitation effects (Fig. 7). These residues show a wide distribution of microenvironmental states. However, the blue shift is reduced because acrylamide is unable to efficiently quench the subpopulations of tryptophans that contribute to the longer wavelengths. The resolution of movement on the nanosecond time scale reveals marked differences between W99 and other buried tryptophans. In contrast, for other residues (e.g. W101 and W103), the amplitude of the induced blue shift is commensurate with that of the red edge effect. We surmize that there is greater accessibility of acrylamide for the subset of microenvironmental states of these tryptophans that fluoresce at longer wavelengths. Therefore, the motion detected for W99 (surrounding dipoles) is not accompanied by increased accessibility to acrylamide but the motion observed in W101 and W103 is accompanied by accessibility to acrylamide. Subtle dynamic changes in accessibility of individual residues may occur during ligand binding and are detectable by SDTF.

The SDTF studies have added insights into the solution structure of the G strand of tear lipocalin. A twisted β sheet structure is apparent. The strand spans the depth of the cavity with exposed residues (L105) that lie at the mouth as well as residues buried deep in the cavity (F99). Polar side chain interactions are apparent (H96). The motion of surrounding dipolar groups for each residue is discernible on the nanosecond time scale. The results suggest that SDTF may be

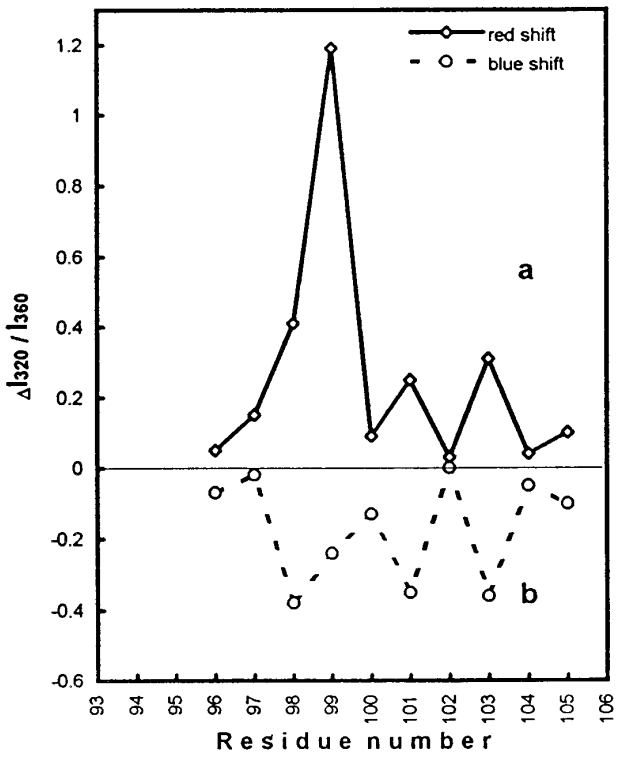

FIG. 7. Red edge excitation and acrylamide induced blue shift effects at the positions of tryptophan substitution in tear lipocalin. **(A)** $\Delta I_{320}/I_{360}$ was calculated from Fig. 6 as the difference in values at excitation wavelengths 295 and 305. **(B)** $\Delta I_{320}/I_{360}$ is the difference of the values in Fig. 6B of acrylamide at 0 and 0.7M.

applicable to other systems. Since the florescence of Trp (emission maximum and quantum yield) is very sensitive to interactions with ligands, SDTF may be especially useful to investigate ligand binding.

ACKNOWLEDGMENTS

This work was supported USPHS NIH EY 11224 and an unrestricted grant from Research to Prevent Blindness to B. J. Glasgow.

REFERENCES

1. Glasgow, B. J., Abduragimov, A. R., Farahbakash, Z., Faull, K. F., and Hubbell, W. G. (1995) *Curr. Eye Res.* **14,** 363–372.
2. Flower, D. R. (1996) *Biochem. J.* **318,** 1–14.
3. Papiz, M. Z. et al. (1986) *Nature* **324,** 383–385.
4. Molinari, H. et al. (1996) *FEBS Letters* **381,** 237–243.
5. Monaco, H. L. et al. (1987) *J. Mol. Biol.* **197,** 695–706.
6. Redl, B., Holzfeind, P., and Lottspeich, F. (1992) *J. Biol. Chem.* **267,** 20282–20287.
7. Huber, R. et al. (1987) *J. Mol. Biol.* **198,** 499–513.
8. Holden, H. M., Rypniewski, W. R., Law, J. H., and Rayment, I. (1987) *EMBO J.* **6,** 1565–1570.
9. Primrose, W. U. (1993) *in* NMR of Macromolecules (Roberts, G. C. K., Ed.), pp. 7–33 Oxford Univ. Press, NY.
10. Altenbach, C., Marti, T., Khorana, H. G., and Hubbell, W. L. (1990) *Science* **248,** 1088–1092.
11. Farrens, D. L., Altenbach, C., Yang, K., Hubbell, W. L., and Khorana, H. G. (1996) *Science* **274,** 768–770.
12. Hubbell, W. L., Mchaourab, H. S., Altenbach, C., and Leitzow, M. A. (1996) *Structure* **4,** 799–783.
13. O'Neil, K. T., Wolfe, H. R., Jr., Erickson-Viitanen, S., and Degrado, W. F. (1987) *Science* **236,** 1454–1456.
14. Weitzman, C., Consler, T. G., and Kaback, H. R. (1995) *Protein Science* **4,** 2310–2318.
15. Locke, B. C., MacInnis, J. M., Qian, S. et al. (1992) *Biochemistry* **31,** 2376–2383.
16. Cai, K., and Schirch, V. (1996) *J. Biol. Chem.* **271,** 2987–2994.
17. Pittman, I., IV, Nakagawa, S. H., Tager, H. S., and Steiner, D. F. (1997) *Biochemistry* **36,** 3430–3437.
18. Eftink, M. R., et al. (1996) *Biochemistry* **35,** 8084–8094.
19. Lakowicz, J. R. (1983) Principles of Fluorescence Spectroscopy, Plenum Press, New York.
20. Eftink, M. R., and Ghiron, C. A. (1976) *Biochemistry* **15,** 672–680.
21. Burstein, E. A., Vedenkina, N. S., and Ivkova, M. N. (1973) *Photochem. Photobiol.* **18,** 263–279.
22. Glasgow, B. J., Heinzmann, C., Kojis, T., Sparkes, R. S., Mohandas, T., and Bateman, J. B. (1993) *Curr. Eye Res.* **11,** 1019–1023.
23. Glasgow, B. J. (1995) *Graefe's Arch Clin Exp Ophthalmol.* **233,** 530–531.
24. Cormack, B. (1987) *in* Current Protocols in Molecular Biology (Ausubel, F. M., Ed.), Suppl. 15, pp. 8.5.1–8.5.9, Greene and Wiley-Interscience, New York.
25. Marston, F. A. O (1987) *in* DNA Cloning, Volume III, A Practical Approach (Glover, D. M., Ed.), pp. 62, IRL Press, Oxford, England.
26. Bozimowski, D., Artiss, J. D., and Zak, B. (1985) *J. Clin. Chem. Clin. Biochem.* **23,** 683–689.
27. Chen, R. F. (1967) *Anal. Lett.* **1,** 3542.
28. Lehrer, S. S. (1971) *Biochemistry* **10,** 3254–3263.
29. Demchenko, A. P. (1988) *Eur. Biophys. J.* **16,** 121–129.
30. Lakowicz, J. R., and Keating-Nakamoto, S. (1984) *Biochemistry* **23,** 3013–3021.